Materials Letters 65 (2011) 3061–3063

Contents lists available at ScienceDirect

Materials Letters

journal homepage: www.elsevier.com/locate/matlet

Tungsten oxide nanoparticles grown by condensation in gas using domestic appliances

V.M. Fuenzalida, D.G. Galvez-Arancibia, I.J. Olavarria-Contreras, M.A. Salinger-Basterrica, D.E. Diaz-Droguett *

Departamento de Física, FCFM, Universidad de Chile, Av. Blanco Encalada 2008, 8370449, Santiago, Chile

ARTICLE INFO

Article history:
Received 17 May 2011
Accepted 26 June 2011
Available online 1 July 2011

Keywords:
Tungsten oxide
Nanoparticles
Gas condensation
Microwave
Light bulbs

ABSTRACT

We report on the preparation of WO_3 nanostructures using tungsten wire and iron wool in a domestic microwave oven. Pure WO_3 nanoparticles were octahedral or rhombohedral while iron containing nanoparticles were spheroidal. Nanoparticles of monoclinic and cubic WO_3 were found in the interior of burned commercial light bulbs, where they grow by a spontaneous reactive gas condensation process. This process was emulated heating a W filament under N_2 inside a glass bell jar with a small air leak.

1. Introduction

Tungsten oxide WO_3 exhibits monoclinic, triclinic, and other structures. There are suboxides, such as $W_{18}O_{49}$, $W_{18}O_{47}$, $W_{20}O_{58}$, $W_{40}O_{118}$, as well as the Magneli phases W_nO_{3n-1} and W_nO_{3n-2} [1]. Tungsten oxides can grow as nanorods, nanoparticles and occasionally nanotubes. Heating a tungsten filament in oxygen leads to the growth of nanoparticles from 10 to 200 nm, generally crystalline and predominantly WO_3 [2]. Heating a tungsten filament in a vacuum chamber with a small air leakage leads to wires standing straight on the filament, around 30 nm in diameter and up to a few tens of micrometers long [3]. Thermal evaporation of tungsten in the presence of oxygen at 1400–1450 °C leads to nanowire networks of WO_{3-x} [4]. A tungsten pellet heated in synthetic air at 1300 Pa, grew 6 nm WO_3 particles of tetragonal structure onto a substrate [5]. Thermal evaporation has been used to prepare nanorods of $W_{18}O_{49}$ in a monoclinic phase, grown directly on a tungsten tip [6,7]. Heating tungsten tips in an oven at atmospheric pressure under different gas mixtures lead to nanostructured tungsten oxides on the tips [8]. Infrared heating tungsten filaments in air coated a silicon substrate placed 2 mm away with WO_3 single crystal nanorods [9].

Evaporation of WO_3 in ultrahigh vacuum onto Al_2O_3 crystals with (0001), (−2110) and (−1102) orientation leads to WO_2 nanoclusters with preferential orientation (10–1) [10]. Vapor transport from a WO_3 layer produced WO_3 nanorods [11]; WO_3 one dimensional nanostructures were prepared sublimating WO_3 in air at atmospheric pressure [12].

Most experiments generate nanoparticles through the gas condensation method [13]. After achieving supersaturation, molecules cool down by collisions with the gas, generating nanoparticles via homogeneous nucleation. We report on the occurrence of this process in domestic appliances, either unintentionally or used purposely for this application.

2. Experimental

2.1. Spontaneous nanoparticle growth

Domestic lightning was often provided by bulbs with tungsten filaments, filled with an inert gas mixture. Normally failure of the lamp occurs through a burst. In a few cases, the failure is slower, with the surface of the lamp turning opalescent, in a process lasting from a few seconds to minutes. We interpret this failure as caused by a tiny leak allowing air into the bulb. The surface of the heated tungsten filament oxidizes and tungsten oxide, gaseous at the temperature of the filament, evaporates. The conditions in the lamp reproduce those found in laboratory gas condensation experiments and are quite similar to several of the experimental setups reviewed; therefore the growth of nanoparticles under these conditions should not be a surprise.

The deposit on the surface of a few lamps burned as described above was scratched, mixed with isopropanol and agitated ultrasonically, putting a drop on a microscope grid and examined by

* Corresponding author at: Departamento de Física, Facultad de Física, Pontificia Universidad Católica de Chile, Santiago, Chile. Tel.: +56 2 354 1681; fax: +56 2 552 6468.
E-mail address: dodiaz@fis.puc.cl (D.E. Diaz-Droguett).

0167-577X/$ – see front matter © 2011 Elsevier B.V. All rights reserved.
doi:10.1016/j.matlet.2011.06.099

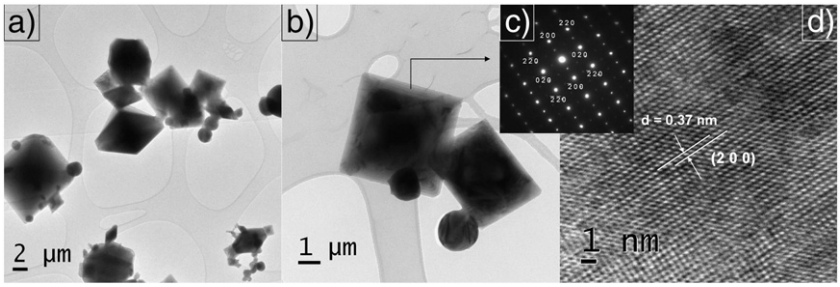

Fig. 1. TEM images of WO_3 particles found inside the bulb: (a) different morphologies and sizes (b) octahedric and spherical particles (c) SAED and (d) HRTEM image.

transmission electron microscopy (TEM) and selected area electron diffraction (SAED).

Fig. 1 shows the material scratched from the bulb. Particles of different sizes and well-defined morphologies such as octahedral, rhombohedral and spherical are identified in Fig. 1. Electron diffraction from different particles revealed monoclinic or cubic WO_3. Fig. 1b shows particles in a strong diffraction condition. The SAED pattern (Fig. 1c) recorded from the largest particle shows its single crystalline character and the indexing of the diffraction spots revealed cubic WO_3. Fig. 1d is a high resolution TEM image recorded from the same particle showing lattice planes with spacing of 0.37 nm, matching the (200) interplanar distance of cubic WO_3.

2.2. Emulation of the light bulb in the laboratory

The conditions inside the bulb were reproduced evacuating a glass bell jar to below 7 Pa and afterwards filling it with nitrogen at pressures of 4000 Pa, 9000 Pa and 54000 Pa. A tungsten filament was resistively heated and a small air flow was allowed to leak into the system. During the experiment the surface of the glass bell jar turned opalescent and after opening the system the powder was collected from the chamber.

The powder, as analyzed by Energy Dispersive X-ray Spectrometry (EDS, not shown), exhibited signals from carbon, copper, oxygen and tungsten. The first two are attributed to the composition of the grid supporting the sample, and the last two to the tungsten oxide, with no other contamination. X-Ray Photoelectron Spectroscopy (XPS) measurements corroborated that the sample did only contain tungsten and oxygen, besides the usual carbon contamination, as shown in Fig. 2. The inset shows a curve fit of the 4f level assigning binding energies of 35.6 eV and 37.7 eV to the W $4f_{7/2}$ and W $4f_{5/2}$ peaks, respectively. These binding energies correspond to +6 state of W indicating the presence of WO_3 [14].

X-ray diffraction was performed on all samples, as shown in Fig. 3. The reflections of the samples coincide with those of monoclinic WO_3 for the three pressures, even collecting the powder from two different locations, the base-plate and the walls of the glass bell jar.

Finally, the TEM micrographs shown in Fig. 4a prove that the sample grown at 9000 Pa of N_2 consisted of WO_3 nanoparticles. The image reveals also some characteristic morphologies of WO_3 grown by gas condensation: octahedral and rhombohedra are identified. The inset is a high resolution image taken from another zone which shows

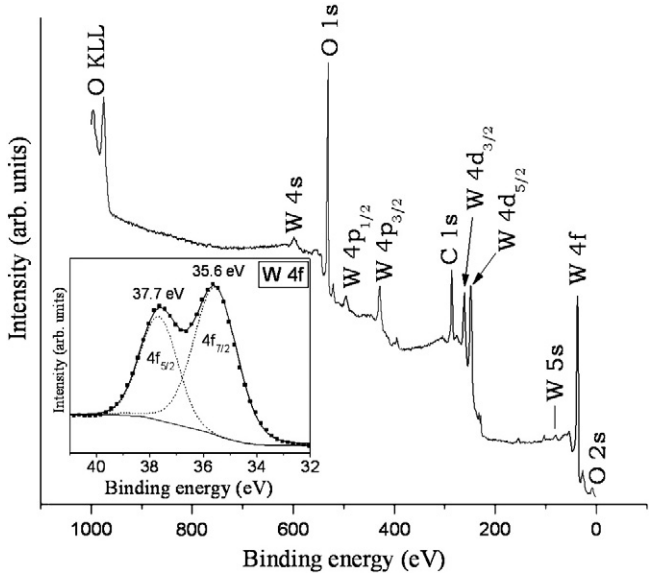

Fig. 2. XPS spectra of a sample grown at a starting pressure of 9000 Pa of N_2: The main picture is a broad energy scan and the inset corresponds to the 4 f level.

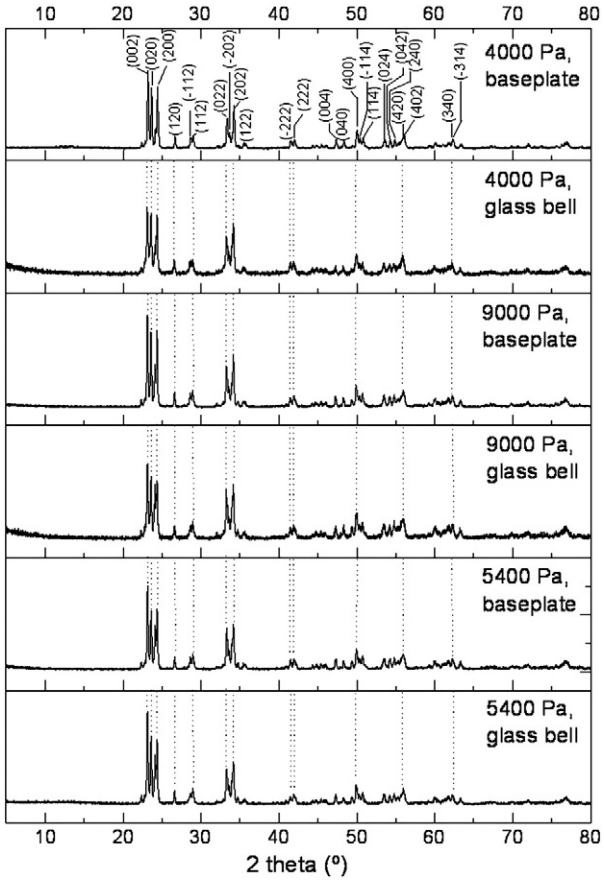

Fig. 3. Diffractograms of WO_3 nanopowder collected from a simulated light bulb with the starting N_2 pressure and origin of the sample indicated in the inset.

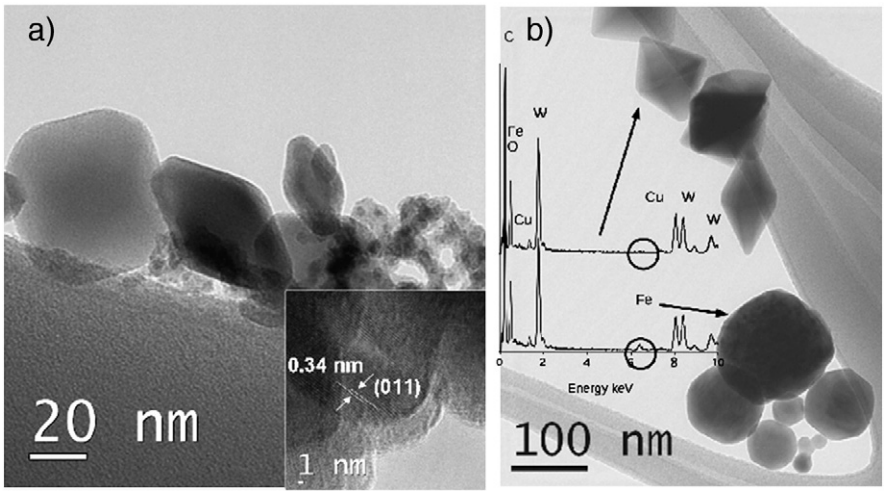

Fig. 4. a) TEM images of WO_3 nanoparticles from a sample grown by reactive thermal evaporation at 9000 Pa of N_2. The inset is a HRTEM image showing the lattice fringes. b) TEM image and EDS spectra of a sample generated inside a microwave oven.

lattice fringes of overlapped particles. The spacing of 0.34 nm corresponds to the interplanar distance between (011) planes of monoclinic WO_3.

2.3. Growth of tungsten oxide nanoparticles in a domestic microwave oven by microwave plasma

Microwave ovens are often used to rapid heating of solutions, leading to fast chemical reactions. Here we restrict to their use in the gas phase, a process often called microwave plasma. MgO [15] and ZnO [16] nanostructures were prepared by putting equal quantities of steel–wool and either magnesium chip or zinc powder in an alumina crucible with a cover in the spot of a microwave oven operated at 1 kW for 30 s. This leads to cubic MgO nanocubes and hexagonal ZnO in the form of nanofibers around 50 nm in diameter and up to 1 mm in length. EDS measurements on the nanostructures only showed Mg or Zn and oxygen. Sullivan et al. [17] were able to reduce RuO_2 to ruthenium microwires using a microwave oven. A similar reduction effect from WO_3 to a/b nanostructured tungsten under microwave irradiation was observed by Murugan et al. [18].

We performed similar experiments by putting a mixture of 0.4 g tungsten wire of 0.1 mm in diameter and 1 g steel wool in a vessel in the focus of a 800 W microwave oven, operated for 30 s. The powder deposited on the surfaces was collected and analyzed by XPS, EDS and TEM.

Fig. 4b) is a typical TEM image of the collected powder showing two groups of nanoparticles. The insets are EDS spectra acquired from each group, as indicated by the arrows. Carbon and copper signals in both spectra are due to the TEM grid. Only oxygen and tungsten were detected by EDS from the rhombohedral particles collected from the top zone, whereas iron was additionally detected from the spheroidal particles collected from the bottom. This is different to the magnesium and zinc based experiments where no contamination of iron was detected by EDS [15,16]. This could be related to the fact that the magnesium and zinc oxidize easier than iron.

The SAED patterns (not shown) from the octahedral and rombohedral nanoparticles (upper zone) revealed monoclinic WO_3.

3. Discussion and conclusions

Nanostructured WO_3 can be produced using domestic appliances by a combination of reactive and inert gas condensation process. In the case of light bulbs, the process is spontaneous, producing monoclinic or cubic WO_3, while the laboratory emulation of the process only produces the monoclinic phase. We temptatively attribute this difference to the (non controlled) temperature of the filament in the light bulb as well as to the different geometry, which affect the convection conditions and thus the cooling rate.

Pure WO_3 nanoparticles grown in a microwave oven were rhomboidal, whereas nanoparticles contaminated with iron were spheroidal and with less defined growth habit. This structural difference respect to the particles grown in the bulb is attributed to conditions far from equilibrium in the microwave, which include arch discharges and plasma formation with high local temperatures and cooling rates.

It is not clear to which extent domestic growth of nanoparticles can have an environmental impact. Microwave ovens are not normally used to heat metals and the operator is warned not to do so (but that some ceramics are decorated with metal, leading to unintentional local overheating). Even if a small fraction of the bulbs in the XX century burned as described here, with low yield, this caused a huge amount of nanoparticles. They are, however, constrained to the bulbs, in tiny amounts, and in a form that does not spread easily (actually they tend to agglomerate).

Acknowledgments

Work financed by the Chilean government under contracts FONDECYT 1070789, 1110168 and UCH0205.

References

[1] Rao CNR, Gopalakrishnan J. New Directions in Solid State Chemistry. Cambridge: Cambridge University Press; 1986.
[2] Mahan AH, Parilla PA, Jones KM, Dillon AC. Chem Phys Lett 2005;413:88–94.
[3] Liu K, Foord DT, Scipioni L. Nanotechnology 2005;16:10–4.
[4] Ponzoni A, Comini E, Sberveglieri G, Zhou J, Deng SZ, Xu NS, et al. Appl Phys Lett 2006;88:23101–3.
[5] Solis JL, Hoel A, Lantto V, Granqvist CG. J Appl Phys 2001;89:2727–32.
[6] Kichambare P. JOM 2005;57:57–9.
[7] Gu G, Zheng B, Han WQ, Roth S, Liu J. Nano Lett 2002;2:849–51.
[8] Zhang H, Feng M, Liu F, Liu L, Chen H, Gao H, et al. Chem Phys Lett 2004;389:337–41.
[9] Li YB, Bando Y, Golberg D, Kurashima K. Chem Phys Lett 2003;367:214–8.
[10] Masek K, Nemsak S, Matolin V. Vacuum 2005;80:58–63.
[11] Guillet M, Delamare R, Gillet E. European Physical Journal D 2005;34:291–4.
[12] Guillet M, Delamare R, Gillet E. J Cryst Growth 2005;279:93–9.
[13] Granqvist CG, Buhrman RA. J Appl Phys 1976;47:2200–19.
[14] Sun M, Xu N, Cao YW, Yao JN, Wang EG. J Mater Res 2000;15:927–33.
[15] Takahashi N. Solid State Sci 2007;9:722–4.
[16] Takahashi N. Mat Lett 2008;62:1652–4.
[17] Sullivan J, Worsley D. Mat Sci and Tech 2009;25(1):121–4.
[18] Murugan K, Chandrasekhar SB, Joardar J. Int J Refract Met Hard Mater 2011;29:128–33.